

FIG. 2. Exploded view of the mechanical resonator, which is made from three pieces of sapphire. The signal mode is the first bending mode of the rectangular section of the middle piece. This piece is clamped between two disks, whose raised edges fix the spacing between capacitor electrodes to be $24 \mu\text{m}$. The thin film electrodes are shown as shaded areas, and have the same labels as in Fig. 1. The *c* electrode is on the underside of the middle piece.

perform a BAE measurement. The phases ϕ, θ of the two pump frequencies are also controllable.

The first experiments were performed using the forcing capacitor in Fig. 2 to apply an oscillating force to the mechanical resonator exactly at its resonant frequency, thus placing it in a state with fixed X_1 and X_2 . The resulting

values of Q_1 and Q_2 were found by amplifying the voltage across the inductor with a GaAs transistor (GAT),⁵ and then demodulating that signal with a two-phase lock-in detector whose reference frequency was f_2 . This was repeated for different values of the phase of the force, relative to the pump, thus producing the succession of states shown in the X -plane diagram within Fig. 3. The corresponding succession of responses in the Q plane was recorded by taking a multiple-exposure oscilloscope photograph of the lock-in outputs for each particular value of f, ϕ , and θ .

We can interpret the results of Fig. 3 as a graphic demonstration of the types of linear coupling discussed by Caves.⁶ The parametric upconverter case ($f=1$) is a faithful and "phase-preserving" mapping onto the Q plane. The two param cases ($f=-1$) are also faithful but "phase-conjugate" mappings onto Q . The two BAE cases ($f=0$) are "phase sensitive" in the sense that information about *only one* of the two components of X is communicated to Q . This is a consequence of the fact that the mapping caused by the coherent superposition of two types of pumping is the vector sum of the individual mappings.

In the second set of experiments we tested the frequency and loss dependence of the parametric coupling of X to Q . To do this we used a pump voltage of the form

$$V_p(t) = V_0 \cos(2\pi f_p t) \quad (2)$$

We recorded the rms magnitude of the lock-in outputs, with its effective reference frequency equal to $f_1 + f_p$, and swept the pump frequency f_p . The predicted response is the superposition of two Lorentzians centered at $f_p = f_2 + f_1$ and $f_2 - f_1$.⁷ In Fig. 4 the calculated and experimental results are shown for two different values of the idler-mode quality factor. The quality factors used to calculate the theoretical curves were determined independently by measuring the relaxation time of the idler mode.

In a third set of experiments we determined the absolute

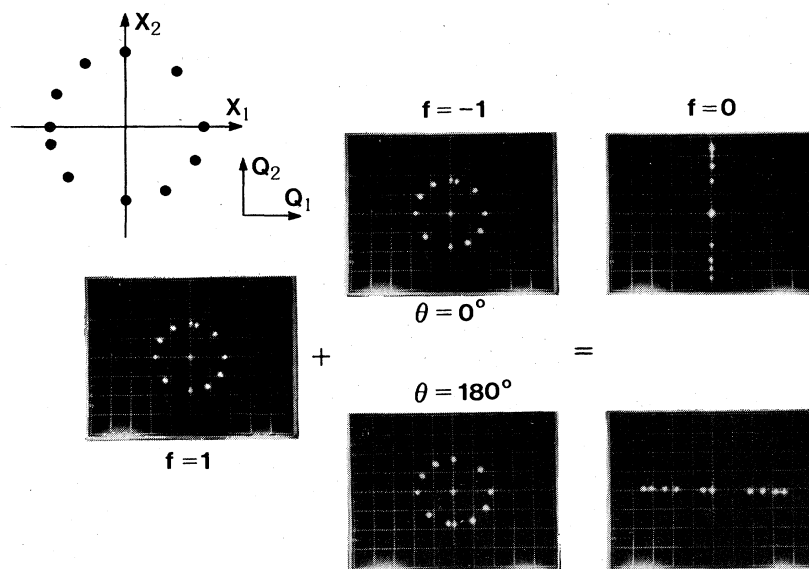


FIG. 3. Oscilloscope photographs of several different steady-state mappings of the diagrammed sequence of X -plane states onto the Q plane. The pump parameters f and θ , defined in the text, determine the character of the mappings. The three mappings on the left convey equal information about both components of the mechanical motion. The two mappings on the right convey information about only one such component. This phase sensitivity is characteristic of a BAE measurement.

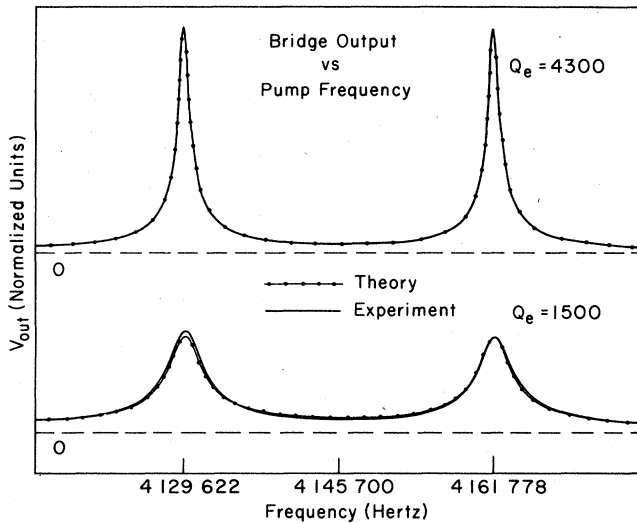


FIG. 4. Test of the frequency and electrical loss dependence of the forward-transfer characteristics. The mean-square output is plotted as a function of the frequency of a single pump [Eq. (2)], for cases where the mechanical mode has a fixed amplitude. The only adjustable parameter in the calculation was the output scale factor. In the top curve, the experimental results and the calculation are indistinguishable.

magnitude of the parametric coupling. To do this we calculated the absolute magnitude of the steady-state displacement amplitude of the mechanical resonator for a given voltage amplitude (V_{CAL}) on the forcing capacitor. This requires knowledge of the shape of the displacement eigenfunction of the signal mode, the forcing capacitor geometry, and the mechanical quality factor. The expected steady-state lock-in output can then be calculated using our knowledge of the pump voltage magnitude V_0 , the electrical quality factor, and the amplifier gains. These results are compared to the measured output values in Fig. 5.

The measured sensitivity was found to have the expected functional dependences but was consistently 52% of the calculated value. We believe that this discrepancy is not due to any fundamental deficiency in the model but is probably due to systematic errors in the determination of V_{CAL} and V_0 , which was greatly complicated by the presence of parasitic impedances. A 25% error in V_{CAL} would account for the disagreement. This seems especially likely since an independent but indirect determination of the sensitivity, obtained by measuring V_{PSD} as a function of a known static capacitance imbalance, yielded a sensitivity that was 89% of the model prediction.

In summary, we have performed the first detailed measurements of the way in which a phase-sensitive transducer

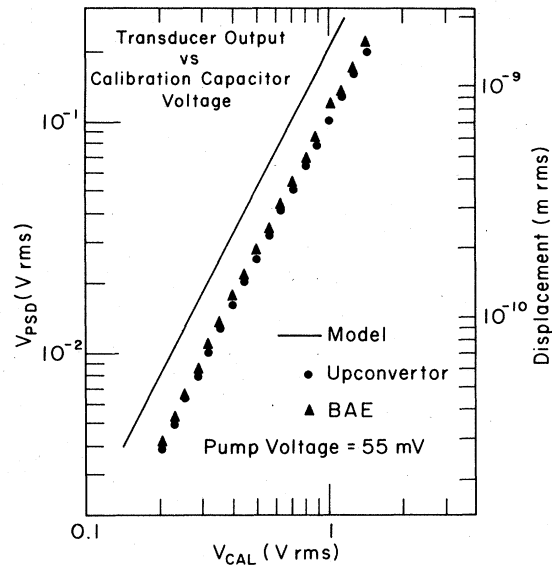


FIG. 5. Test of the absolute magnitude of the forward-transfer characteristics. The rms output of the lock-in (V_{PSD}) is plotted vs the forcing capacitor voltage (V_{CAL}) for two different types of pumping. All the parameters in the calculated response (labeled Model) are determined by independent measurements. The discrepancy is believed to be due to systematic errors, as discussed in the text. The right-hand scale shows the calculated displacement amplitude for the data points.

transforms a mechanical input into an electrical output. All these results are consistent with the predictions that can be derived from the proposed equations of motion for this system.^{1,3,7} What remains to be done is just as important: make careful measurements of the noise properties of this transducer.

The transducer described in this paper offers two exciting possibilities. First, we believe it is an excellent candidate as the transducer on massive gravitational wave detectors. With currently achievable parameters, the use of back action evasion is estimated to increase the energy sensitivity of detectors by a factor of 10–100.⁸ Second, the model predicts that the quantum-noise limit may be reachable with current technology and possibly exceeded by use of BAE. When this level of sensitivity is reached questions concerning the quantum theory of measurement may be directly tested in a unique way, by repeated measurements on a single macroscopic body.

We would like to acknowledge discussions with David H. Douglass. This work was supported by the National Science Foundation.

¹W. W. Johnson and M. F. Bocko, *Phys. Rev. Lett.* **47**, 1184 (1981).

²C. M. Caves, K. S. Thorne, R. W. P. Drever, V. D. Sandberg, and M. Zimmermann, *Rev. Mod. Phys.* **52**, 341 (1980).

³M. F. Bocko and W. W. Johnson, *Phys. Rev. Lett.* **48**, 1371 (1982).

⁴V. B. Braginsky, Yu. I. Vorontsov, and K. S. Thorne, *Science* **209**, 547 (1980).

⁵M. F. Bocko, *Rev. Sci. Instrum.* **55**, 256 (1984).

⁶C. M. Caves, *Phys. Rev. D* **26**, 1817 (1982).

⁷M. F. Bocko, Ph.D. thesis, University of Rochester, 1984.

⁸M. F. Bocko, L. Narici, D. H. Douglass, and W. W. Johnson, *Phys. Lett.* **97A**, 259 (1983).

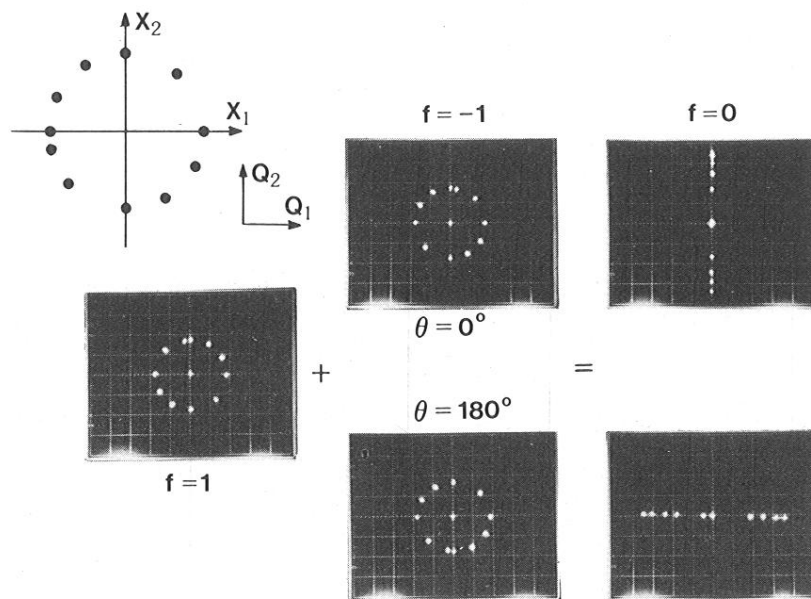


FIG. 3. Oscilloscope photographs of several different steady-state mappings of the diagrammed sequence of X -plane states onto the Q plane. The pump parameters f and θ , defined in the text, determine the character of the mappings. The three mappings on the left convey equal information about both components of the mechanical motion. The two mappings on the right convey information about only one such component. This phase sensitivity is characteristic of a BAE measurement.